Kondo screening of single magnetic impurity doped type-II Ising superconductors

Shi-Nan Chen,[1] Jin-Hua Sun,[2,*] Zhen-Hua Wang,[1] Wei Su,[1,3] Dong-Hui Xu,[4,5] Hong-Gang Luo,[6,7] and Lin Li[1,†]

[1]*Department of Physics and Electronic Engineering, and Center for Computational Sciences, Sichuan Normal University, Chengdu, 610068, China*

[2]*Department of Physics, Ningbo University, Ningbo 315211, China*

[3]*Beijing Computational Science Research Center, Beijing 100084, China*

[4]*Department of Physics and Chongqing Key Laboratory for Strongly Coupled Physics, Chongqing University, Chongqing 400044, China*

[5]*Center of Quantum Materials and Devices, Chongqing University, Chongqing 400044, China*

[6]*School of Physical Science and Technology Lanzhou University, Lanzhou 730000 China*

[7]*Lanzhou Center for Theoretical Physics and Key Laboratory of Theoretical Physics of Gandhi Province, Lanzhou University, Lanzhou 730000, China*

(Received 10 October 2022; revised 28 December 2022; accepted 31 January 2023; published 8 February 2023)

We theoretically study the Kondo effect in type-II Ising superconductors with a single magnetic impurity. Type-II Ising superconductivity was found in two-dimensional centrosymmetric materials with multiple degenerate orbitals, such as in few-layer stanene [Falson *et al.*, Science **367**, 1454 (2020)] and ultrathin $PdTe_2$ films [Liu *et al.*, Nano Lett. **20**, 5728 (2020)]. The type-II Ising spin-orbit coupling (SOC) in these materials generates out-of-plane effective Zeeman fields orienting opposite directions for opposing orbitals, which strongly protects the interorbital superconducting pairing states against in-plane magnetic fields. We show that the SOC-induced band splitting and the chemical potential significantly influence the formation of a localized magnetic moment, with particle-hole asymmetry in the phase boundary between magnetic and nonmagnetic states. The behaviors of spin-induced Yu-Shiba-Rusinov bound states and low-temperature magnetic susceptibility demonstrate that the SOC suppresses the Kondo screening of the magnetic moment, while the interorbital mixing weakens the SOC at finite momentum, then enhances the Kondo effect. The quantum phase transition between magnetic doublet and Kondo singlet ground states can be tuned through chemical potential in experiments.

DOI: 10.1103/PhysRevB.107.075115

I. INTRODUCTION

The emergence of two-dimensional (2D) superconductivity in atomic layer materials and interfaces has attracted tremendous research interest due to fundamental physics and potential applications [1–6]. 2D superconductors exhibit numerous interesting properties, such as localization of Cooper pairs [7], quantum size effect induced transition-temperature oscillation [8,9], and Berezinskii-Kosterlitz-Thouless transition [10,11]. The breaking of in-plane inversion symmetry in monolayer transition metal dichalcogenides (TMDs) generates an Ising-type spin-orbit coupling (SOC) which locks the spins of pairing electrons at opposite valleys to the out-of-plane directions. As a result, the in-plane upper critical magnetic field of Ising superconductors far exceeds the Pauli paramagnetic limit [2–4,12,13]. More recently, another class of Ising superconductors, dubbed type-II Ising superconductors, have been predicted in 2D centrosymmetric materials with multiple degenerate orbitals [14], and subsequently observed in few-layer stanene and ultrathin $PdTe_2$ films [15,16]. In these materials, the SOC splits the fourfold degenerate orbitals $p_{x,y}$ into two sets of spin-degenerate bands $p_x \pm ip_y$ near the Γ point and polarizes the spins along the out-of-plane direction, thus protecting the superconducting pairing between carriers with opposite spins and orbitals against in-plane magnetic fields.

Magnetic impurities have a dramatic impact on superconductivity, which in turn provides a useful tool to explore the fundamental properties of superconductors [17–20]. In a superconductor containing magnetic impurities, the exchange coupling between magnetic moment and Cooper pairs generates the in-gap Yu-Shiba-Rusinov (YSR) bound states [21–23]. The YSR states can reveal interesting physics derived from the competition between Kondo effect and pairing interactions [24–30]. The Kondo effect, scaled by the Kondo temperature T_K, originates from the screening of the magnetic moment by conduction electrons near the Fermi level [31]. However, the Kondo screening would be suppressed by superconducting pairing interaction due to the formation of energy gap Δ [20,24,25]. When the pairing interaction dominates over the Kondo effect, $\Delta \gg T_K$, the ground state is a magnetic doublet state. In the opposite limit, $\Delta \ll T_K$, the ground state is a Kondo screened singlet state. The quantum phase transition (QPT) between the two ground states takes place at $T_K/\Delta \sim 1$, manifesting itself as a level crossing between YSR states [20,24,25,29,32].

In TMD Ising superconductors, Ising-SOC induced band splitting and spin-momentum locking near the K and $-K$ valleys bring unique phenomena to YSR states and Kondo physics [33]. The magnetic impurity induced YSR states are protected by Ising SOC and stay robust to unusually large

*sunjinhua@nbu.edu.cn
†linli2018@sicnu.edu.cn

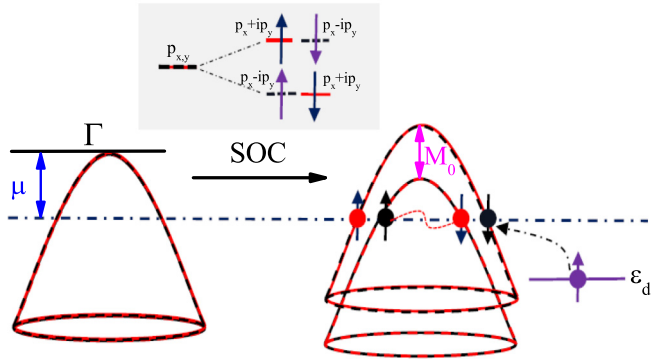

FIG. 1. Schematic diagram of a magnetic impurity doped in type-II Ising superconductors. The fourfold degenerate orbitals $p_{x,y}$ near the Γ point split into two sets of spin-degenerate bands $p_x \pm ip_y$ in the presence of Ising-type spin-orbit coupling (SOC). The superconducting pairing between carriers with opposite spins and orbitals is protected against the in-plane magnetic fields by the Ising SOC induced out-of-plane effective Zeeman field

in-plane magnetic fields [34]. The interplay of Kondo effect and Ising superconductivity depends on the particular band structure near the K $(-K)$ valleys, and the SOC imposes opposite influences on the Kondo screening in the electron- and hole-doped cases [35]. If a ferromagnetic atomic chain is placed on the surface of a monolayer TMD superconductor, the YSR states form a topological superconducting chain, which holds Majorana zero modes at the ends [34,36]. Studies of Kondo physics in type-II Ising superconductors are still lacking. In few-layer stanene and ultrathin $PdTe_2$ films, the Ising-type SOC splits the fourfold degenerate orbitals $p_{x,y}$ into two sets of spin-degenerate bands $p_x \pm ip_y$ as shown schematically in Fig. 1. The Cooper pairs are composed of electrons with opposite spin, momentum, and orbitals near the Γ point, which is sharply contrasted to those in the TMD Ising superconductors. In the present paper, we focus on the Kondo physics of a magnetic impurity doped in type-II Ising superconductors. We show the formation of a localized magnetic moment depends on the SOC as well as the chemical potential, and the phase boundary between the magnetic and nonmagnetic states exhibits particle-hole asymmetry. The Kondo screening of the magnetic moment is suppressed by the SOC but is enhanced by the interorbital mixing of the spin-degenerate bands. Therefore, the band splitting near the Γ point significantly influences the phase transition between the magnetic doublet and Kondo singlet (KS) ground states, which can also be tuned through the chemical potential.

The paper is organized as follows. In Sec. II, we present the model used to study the Kondo effect in type-II Ising superconductors and set out its theoretical treatments. In Sec. III, we discuss the physics dominated by the interplay between Kondo effect and Ising superconductivity based on the behaviors of YSR states and localized magnetic susceptibility. A brief summary is devoted to Sec. IV.

II. MODEL AND FORMALISM

The Hamiltonian of a magnetic impurity doped in type-II Ising superconductors reads

$$H = H_c + H_d + H_V, \tag{1}$$

where

$$H_c = \sum_{km\sigma}[\varepsilon(k) + m\sigma M(k)]c^\dagger_{km\sigma}c_{km\sigma} + \sum_{km}(\Delta c^\dagger_{km\uparrow}c^\dagger_{-k-m\downarrow} + \text{H.c.}) \tag{2}$$

is the $\vec{k}\cdot\vec{p}$ Hamiltonian describing the electron states around the Γ point, as shown in Fig. 1. Here, $\varepsilon(k) = \varepsilon_0 + \varepsilon_1(k_x^2 + k_y^2)$ is the single-particle energy with $\varepsilon_0 = 0$ at the Γ point and the coefficient $\varepsilon_1 = -1$. $M(k) = M_0 - M_1(k_x^2 + k_y^2)$ models the Ising-type SOC in type-II Ising superconductors, with M_0 the SOC strength and M_1 the interorbital mixing strength. $m = \pm 1$ and $\sigma = \pm 1$ correspond to the orbital and spin indices in the basis $(|+,\uparrow\rangle, |+,\downarrow\rangle, |-,\uparrow\rangle, |-,\downarrow\rangle)$, respectively, where $|\pm\rangle$ refers to the $p_x \pm ip_y$ orbitals. Δ is the pairing in two energetically degenerate bands with opposite orbital and spin indices as shown in Fig. 1. Because of the large band splitting induced by the SOC, we neglect the interband mixing term that has been introduced in the $\vec{k}\cdot\vec{p}$ Hamiltonian in Ref. [14]. The Hamiltonian of magnetic impurity is

$$H_d = \sum_\sigma \varepsilon_{d\sigma} d^\dagger_\sigma d_\sigma + U n_{\bar\sigma} n_\sigma, \tag{3}$$

with the impurity level $\varepsilon_{d\sigma}$ and the Coulomb repulsion U. The operator $d^\dagger_\sigma(d_\sigma)$ indicates the creation (annihilation) of an electron on the impurity level, and $n_\sigma = d^\dagger_\sigma d_\sigma$. The coupling between the magnetic impurity and conduction electrons is

$$H_V = \sum_{km\sigma}(V_0 c^\dagger_{km\sigma} d_\sigma + \text{H.c.}), \tag{4}$$

where the coupling amplitude V_0 is assumed to be independent of momentum, orbital, and spin degrees of freedom for simplification.

The ground state of the system described by Eq. (1) could be a BCS singlet, a magnetic doublet, or a KS state, depending on the relative strengths of the characteristic energies of the pairing interaction Δ, the Coulomb repulsion U, and the Kondo temperature T_K [28,30]. Intriguing emergent phenomena dominated by these competitive ground states can be captured by the impurity Green's function (GF)

$$\hat G_{d\sigma}(\omega) = \hat G^0_{d\sigma}(\omega)[1 + U\hat F_{d\sigma}(\omega)], \tag{5}$$

with $\hat G_{d\sigma}(\omega) = \langle\langle \hat\Psi_\sigma; \hat\Psi^\dagger_\sigma\rangle\rangle$ and $\hat\Psi^\dagger_\sigma = (d^\dagger_\sigma, d_{\bar\sigma})$. The noninteracting GF obtained is

$$\hat G^0_{d\sigma}(\omega) = \left[\hat I\omega - \hat\sigma_z \text{diag}(\varepsilon_{d\sigma}, \varepsilon_{d\bar\sigma}) - \hat\Sigma^0_\sigma(\omega)\right]^{-1}, \tag{6}$$

with the components of self-energy $\hat\Sigma^0_{11(22)\sigma}(\omega) = \frac{\Gamma_0}{\pi}\sum_{km}\frac{\omega \pm \varepsilon(k) + \sigma m M(k)}{\omega^2 - [\varepsilon(k)\pm\sigma m M(k)]^2 - \Delta^2}$ and $\hat\Sigma^0_{12(21)\sigma}(\omega) = \frac{\sigma\Delta\Gamma_0}{\pi}\sum_{km}\frac{1}{\omega^2 - [\varepsilon(k)\pm\sigma m M(k)]^2 - \Delta^2}$, $\Gamma_0 = \pi|V_0|^2$ measuring the coupling strength. The notation

$$\hat F_{d\sigma}(\omega) = \begin{pmatrix} \langle\langle d_\sigma n_{\bar\sigma}; d^\dagger_\sigma\rangle\rangle_\omega & \langle\langle d_\sigma n_{\bar\sigma}; d_{\bar\sigma}\rangle\rangle_\omega \\ -\langle\langle d^\dagger_{\bar\sigma} n_\sigma; d^\dagger_\sigma\rangle\rangle_\omega & -\langle\langle d^\dagger_{\bar\sigma} n_\sigma; d_{\bar\sigma}\rangle\rangle_\omega \end{pmatrix} \tag{7}$$

includes some high-order GFs that should be treated properly to capture the underlying physics.

In the frame of Hartree-Fock approximation (HFA), the impurity GF can be approximately given by

$$\hat G_{d\sigma}(\omega) = \hat G^0_{d\sigma}(\omega) + \hat G^0_{d\sigma}(\omega)\hat\Sigma^{\text{HF}}_\sigma(\omega)\hat G_{d\sigma}(\omega), \tag{8}$$

with the interacting self-energy

$$\hat{\Sigma}_{\sigma}^{\mathrm{HF}}(\omega)=U\begin{pmatrix}\langle n_{\bar{\sigma}}\rangle & \langle d_{\bar{\sigma}}d_{\sigma}\rangle\\ \langle d_{\sigma}^{\dagger}d_{\bar{\sigma}}^{\dagger}\rangle & -\langle n_{\sigma}\rangle\end{pmatrix}, \tag{9}$$

where $\langle n_{\bar{\sigma}}\rangle=-\frac{1}{\pi}\int f(\omega)\mathrm{Im}[\hat{G}_{d\bar{\sigma}}(\omega)]_{11}d\omega$ is the occupation of impurity level and $f(\omega)$ is the Fermi distribution function. The pairing correlation function can be calculated by $\langle d_{\sigma}^{\dagger}d_{\bar{\sigma}}^{\dagger}\rangle=-\frac{1}{\pi}\int f(\omega)\mathrm{Im}[\hat{G}_{d\sigma}(\omega)]_{21}d\omega$. Then, the diagonal component of GF can be explicitly written as

$$[\hat{G}_{d\sigma}(\omega)]_{11}=\frac{1}{\omega-\varepsilon_{d\sigma}-\hat{\Sigma}_{11\sigma}^{0}(\omega)-U\langle n_{\bar{\sigma}}\rangle+\hat{\Sigma}_{12\sigma}^{0}(\omega)\Theta_{\sigma}(\omega)}, \tag{10}$$

and the anomalous GF reads

$$[\hat{G}_{d\sigma}(\omega)]_{21}=\Theta_{\sigma}(\omega)[\hat{G}_{d\sigma}(\omega)]_{11}, \tag{11}$$

with

$$\Theta_{\sigma}(\omega)=\frac{U\langle d_{\sigma}^{\dagger}d_{\bar{\sigma}}^{\dagger}\rangle-\hat{\Sigma}_{21\sigma}^{0}(\omega)}{\omega+\varepsilon_{d\bar{\sigma}}+U\langle n_{\sigma}\rangle-\hat{\Sigma}_{22\sigma}^{0}(\omega)}. \tag{12}$$

The HFA can properly characterize the behaviors of the localized magnetic moment [37,38]. It can be used to discuss the phase transition between the BCS singlet and the magnetic doublet ground states [39–42]. However, the HFA fails to describe the Kondo effect at low temperatures [43,44].

To study the Kondo effect of a magnetic impurity doped in type-II Ising superconductors, we take the Lacroix's approximation to treat high-order GFs in $\hat{F}_{d\sigma}(\omega)$ [43–53]. One can refer to the details in the Appendix. After some straightforward calculations, we obtain

$$[\hat{G}_{d\sigma}(\omega)]_{11}=\frac{1+U\Lambda_{\sigma}(\omega)}{\omega-\varepsilon_{d\sigma}-\hat{\Sigma}_{11\sigma}^{0}(\omega)-U\Phi_{\sigma}(\omega)+\Theta_{\sigma}(\omega)}, \tag{13}$$

with the notations

$$\Lambda_{\sigma}(\omega)=\frac{\langle n_{\bar{\sigma}}\rangle+\Pi_{2\sigma}(\omega)-\Pi_{3\sigma}(\omega)}{\omega-\varepsilon_{d\sigma}-U-\Xi_{1\sigma}(\omega)-\Xi_{2\sigma}(\omega)-\Xi_{3\sigma}(\omega)} \tag{14}$$

and

$$\Phi_{\sigma}(\omega)=\frac{[\Pi_{2\sigma}(\omega)-\Pi_{3\sigma}(\omega)]\hat{\Sigma}_{11\sigma}^{0}(\omega)-[\Omega_{2\sigma}(\omega)+\Omega_{3\sigma}(\omega)]}{\omega-\varepsilon_{d\sigma}-U-\Xi_{1\sigma}(\omega)-\Xi_{2\sigma}(\omega)-\Xi_{3\sigma}(\omega)}, \tag{15}$$

where $\Xi_{i\sigma}(\omega)=\frac{\Gamma_0}{\pi}\sum_{km}\frac{1}{\omega-\varepsilon_{im\sigma k}}$ $(i=1,2,3)$, and the symbols are $\varepsilon_{1m\sigma k}=\varepsilon(k)-m\sigma M(k)$, $\varepsilon_{2m\sigma k}=\varepsilon(k)-m\sigma M(k)+\varepsilon_{d\sigma}-\varepsilon_{d\bar{\sigma}}$, and $\varepsilon_{3m\sigma k}=-\varepsilon(k)+m\sigma M(k)+\varepsilon_{d\sigma}+\varepsilon_{d\bar{\sigma}}+U$. Other notations involved in Eqs. (14) and (15) are

$$\Pi_{i\sigma}(\omega)=\frac{\Gamma_0}{\pi}\sum_{km}\frac{\phi_{m\sigma}(k)}{\omega-\varepsilon_{im\sigma k}} \tag{16}$$

and

$$\Omega_{i\sigma}(\omega)=\frac{\Gamma_0}{\pi}\sum_{km}\frac{\varphi_{m\sigma}(k)}{\omega-\varepsilon_{im\sigma k}}, \tag{17}$$

with the symbols

$$\phi_{m\sigma}(k)=\frac{-1}{\pi}\int d\omega f(\omega)\mathrm{Im}\frac{[\omega+\varepsilon(k)-\sigma mM(k)][\hat{G}_{d\bar{\sigma}}(\omega)]_{11}}{\omega^2-[\varepsilon(k)-\sigma mM(k)]^2-\Delta^2} \tag{18}$$

and

$$\varphi_{m\sigma}(k)=\frac{-1}{\pi}\int d\omega f(\omega)\mathrm{Im}\frac{\omega+\varepsilon(k)-m\sigma M(k)}{\omega^2-[\varepsilon(k)-\sigma mM(k)]^2-\Delta^2}. \tag{19}$$

The Lacroix's scheme can qualitatively capture the Kondo physics of the magnetic impurity doped in superconductors [32,53,54]. Because the superconducting correlation at the impurity site is significantly suppressed by the Coulomb repulsion ($U\gg\Delta$), we can safely neglect the high-order correlation terms in nondiagonal components of $\hat{F}_{d\sigma}(\omega)$, and the HFA is good enough to treat the anomalous parts of $\hat{F}_{d\sigma}(\omega)$ [40,41]. One can calculate the impurity GF $\hat{G}_{d\sigma}(\omega)$ with above formulas self-consistently.

III. NUMERICAL RESULTS

We first determine the formation of a local moment in a type-II Ising superconductor within the framework of HFA. A localized magnetic moment forms whenever the impurity level is singly occupied with opposite spins $\langle n_{\sigma}\rangle\neq\langle n_{\bar{\sigma}}\rangle$ [37]. The local density of states and the occupations of impurity level are self-consistent, calculated by Eqs. (8) and (9). The results show that the formation of magnetic moment depends on the SOC when the chemical potential is tuned around the Γ point. The phase boundary between the magnetic and nonmagnetic states exhibits particle-hole asymmetry as shown in Fig. 2(a). The results differ from the symmetric phase diagram obtained for an impurity doped in conventional superconductors [55], where the phase boundary is symmetric about $(\mu-\varepsilon_d)/U=1/2$. Especially, the magnetic state exists even in part of doubly occupied region ($\varepsilon_d+U<\mu$) for $\mu=0$. Here the single and doubly occupied regions imply that the impurity levels are singly ($|\uparrow\rangle$, $|\downarrow\rangle$) and doubly occupied ($|\uparrow\downarrow\rangle$) in the ground states, respectively. The anomalous behavior of localized magnetic moment, extending to empty ($\varepsilon_d>\mu$) or doubly occupied state, has been observed for an impurity doped in graphene or Dirac semimetal due to the lack of density of states near the Dirac point [38,56]. In type-II Ising superconductors, the density of carriers around the Fermi level increases by taking the SOC into consideration. Thus, the magnetic state in doubly occupied region is quenched gradually by the increase of M_0. When the SOC is large enough, e.g., $M_0=10\Delta$, the magnetic moment, as usual, forms merely in singly occupied region ($\varepsilon_d<\mu<$

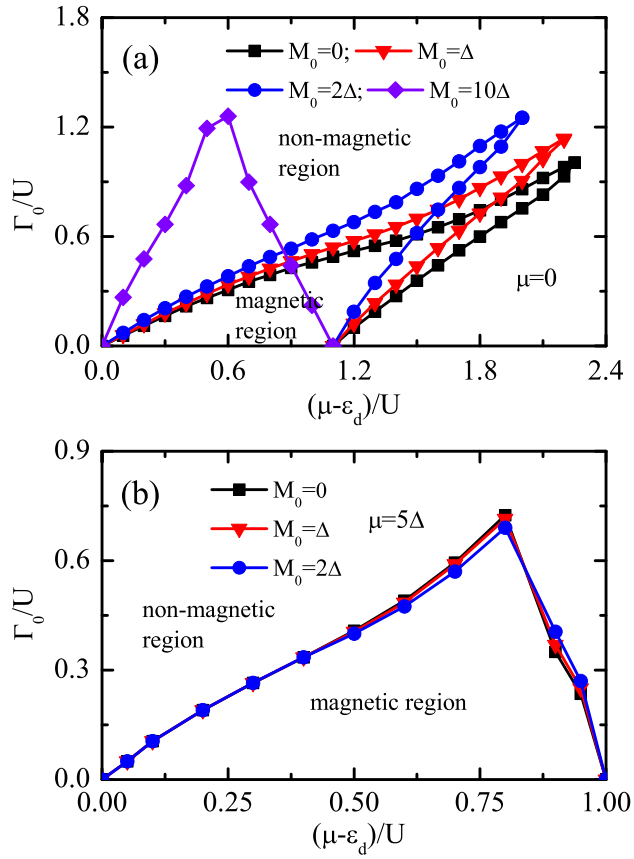

FIG. 2. The magnetic state of an impurity doped in type-II Ising superconductors varying with the coupling Γ_0 and the impurity level ε_d by setting the chemical potential $\mu = 0$ in (a) and $\mu = 5\Delta$ in (b), and the Coulomb repulsion $U = 10\Delta$. The Ising-type SOC is characterized by the parameters $M_0 = 0$, Δ, 2Δ, 10Δ and $M_1 = 0$.

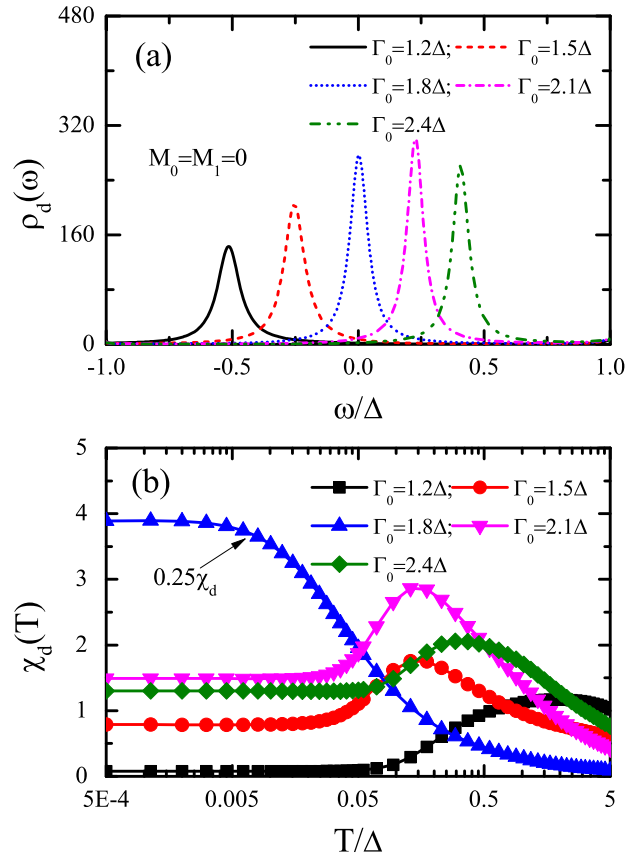

FIG. 3. (a) The quantum phase transition (QPT) between magnetic doublet and Kondo singlet ground states indicated by the level crossing of YSR bound states. (b) The temperature-dependent magnetic susceptibility varying with the coupling strength Γ_0. Other parameters are evaluated with the chemical potential $\mu = 0$, the impurity level $\varepsilon_d = -8\Delta$, the Coulomb repulsion $U = 200\Delta$, and the SOC interactions $M_0 = 0$ and $M_1 = 0$.

$\varepsilon_d + U$). In the nonmagnetic region, the superposition of empty and doubly occupied states constitutes the BCS singlet ground state [55], which is quenched by large Coulomb repulsion at the impurity site. When the Fermi level is tuned well below the Γ point, e.g., $\mu = 5\Delta$, the magnetic state, as in normal metal with parabolic dispersion, exists only in singly occupied region; see Fig. 2(b). In this case, the SOC has no obvious influence on the formation of a localized magnetic moment. Asymmetry in the phase boundary between magnetic and nonmagnetic states originates from the breaking of hole-particle symmetry in the bands. The interorbital mixing process characterized by M_1 plays as a role to weaken the effects induced by SOC at finite k [15].

We now focus on the magnetic region and discuss the Kondo screening of a magnetic impurity doped in a type-II Ising superconductor based on the Lacroix's approximation. First, we study the interplay between Kondo effect and superconductivity in the absence of Ising SOC. Then, we explore the roles played by the Ising SOC in the Kondo physics. The Kondo effect in a superconductor can be characterized by the spin-induced YSR bound states in the local density of states $\rho_d(\omega) = -\frac{1}{\pi}\Sigma_\sigma \mathrm{Im}[G_{d\sigma}(\omega)]_{11}$ [20,25,29,54]. In Fig. 3(a), we explore the evolution of YSR state by increasing the coupling strength Γ_0. When $\Gamma_0 < 1.8\Delta$, the YSR state is situated below the Fermi level, the ground state is a magnetic doublet (MD) state. By further increasing Γ_0, the YSR bound state is tuned above the Fermi level. Correspondingly, the ground state becomes a KS state. The quantum phase transition between MD and KS ground states occurs around $\Gamma_0 = 1.8\Delta$ when the YSR state crosses the Fermi level [20,29]. To explore the Kondo screening of the localized magnetic moment, we discuss the temperature-dependent magnetic susceptibility, which is defined as $\chi_d(T) = \frac{g\mu_B(n_\uparrow - n_\downarrow)}{h}|_{h\to 0}$ with h a small magnetic filed. In Fig. 3(b), the low-temperature susceptibility is enhanced by increasing the coupling, e.g., $\Gamma_0 = 1.2\Delta, 1.5\Delta, 1.8\Delta$. However, the magnetic susceptibility is suppressed by further increasing the coupling, such as $\Gamma_0 = 2.1\Delta, 2.4\Delta$. The strong coupling between the magnetic impurity and Cooper pairs transfers the local spin to the YSR bound states [21–23]; as a result, the YSR bound states possess effective magnetic moment [53]. In the former case, the effective magnetic moment of the YSR state is developed gradually because of the enhancement of pair-breaking scattering. At the level-crossing phase transition point ($\Gamma_0 \approx 1.8\Delta$), the ratio of the energy scales is $T_K/\Delta \sim 1$ [57]. By further increasing

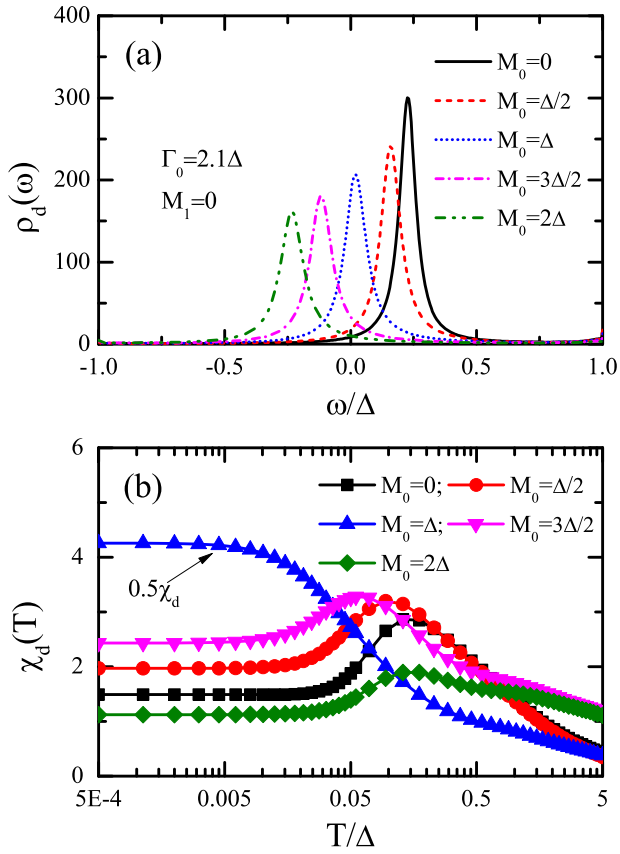

FIG. 4. (a) The level-crossing QPT driven by the SOC interaction M_0 in type-II Ising superconductor. (b) The suppression of Kondo screening indicated by the low-temperature magnetic susceptibility in the presence of SOC. The coupling strength is evaluated with $\Gamma_0 = 2.1\Delta$, and other parameters are taken the same as that in Fig. 3.

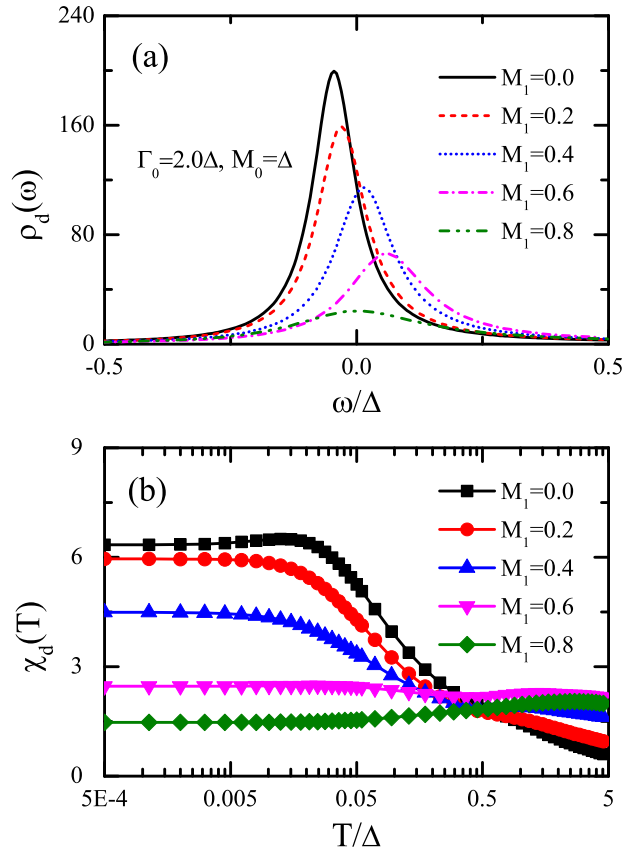

FIG. 5. (a) The interorbital mixing effect enhanced Kondo screening indicated by the shifting and broadening of YSR states. (b) The magnetic susceptibility is suppressed by the increase of M_1. The parameters are evaluated with the coupling strength $\Gamma_0 = 2\Delta$ and the SOC interaction$M_0 = \Delta$, and other parameters taken are the same as that in Fig. 3.

the coupling, the magnetic moment is screened by the Kondo effect, and the ground state becomes a KS state.

In the presence of Ising-type SOC, the fourfold degeneracy of the band is lifted to generate a gap M_0, and the density of carriers near the Γ point decreases. To explore the roles played by the Ising-type SOC, here we neglect the interorbital mixing effect by setting $M_1 = 0$. By tuning the chemical potential with $\mu = 0$, the Kondo screening is suppressed by the SOC due to the decrease of the density of carriers around the Fermi level. As shown in Fig. 4(a), the shifting of YSR states indicates that the ground state of the system is transformed from a KS to a magnetic doublet state by increasing M_0. Consequently, the low-temperature susceptibility is enhanced due to the suppression of Kondo screening of the localized magnetic moment see the lines marked by $M_0 = 0, \Delta/2, \Delta$ in Fig. 4(b). By further increasing the SOC, e.g., $M_0 = 3\Delta/2, 2\Delta$, the magnetic susceptibility is suppressed and the ground state becomes a magnetic doublet because the pair-breaking scattering decreases. Correspondingly, the effective moment of YSR bound states is quenched due to the decrease of the density of carriers.

The interorbital mixing effect, described by the term $M_1(k_x^2 + k_y^2)$ in Eq. (1), plays a part to suppress the SOC-induced band splitting at the finite-k case [14]. Hence, the Kondo screening of the magnetic impurity would be enhanced by taking the interorbital mixing effect into consideration. In Fig. 5(a), we show a phase transition from the magnetic doublet to the KS ground state is induced by increasing M_1. Simultaneously, the width of the YSR state is significantly broadened due to the increase of carrier density near the Fermi level. The interorbital mixing effect enhances the Kondo screening, leading to the suppression of low-temperature susceptibility, as shown in Fig. 5(b).

Besides the influence of SOC, the chemical potential also plays an important role in the Kondo effect because the density of carriers near the Fermi level can be tuned through the chemical potential μ. In Fig. 6, we show the phase diagram dominated by the interplay between the Kondo effect and superconductivity in a hole-doped type-II Ising superconductor as shown schematically in Fig. 1. Here, we neglect the interorbital mixing term $M_1 = 0$, which merely suppresses the influence of SOC in the Kondo effect. When a magnetic impurity is doped in convention s-wave superconductors, the QPT between the magnetic doublet and the KS ground states occurs at $T_K/\Delta \sim 1$ [57]. The normal state Kondo temperature is approximately given by the Haldane's scaling theory $T_K \approx \tilde{\Gamma}\exp(\pi\varepsilon_d/2\tilde{\Gamma})$ [58], where the coupling $\tilde{\Gamma} = \pi\Gamma_0$ is defined independent of the density of carriers. In a type-II Ising superconductor, the critical value of T_K/Δ varying with

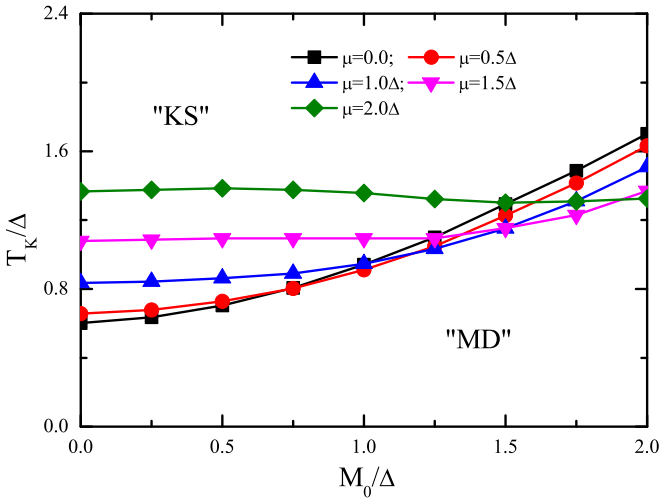

FIG. 6. The phase diagram dominated by the competition between Kondo effect and superconductivity in type-II Ising superconductor. The critical value of T_K/Δ is determined by the chemical potential μ and the SOC M_0 with $M_1 = 0$.

the SOC and chemical potential reflects the influence of the density of carriers around the Fermi level on the Kondo effect. In the lightly doped region, e.g., for $\mu < \Delta$, the parameter T_K/Δ is shown conspicuously increasing with the strength of SOC M_0. The reason is that the SOC-induced band splitting around the Γ point significantly reduces the density of carriers near the dome region, then suppresses the Kondo screening in the superconductor. In the heavily doped region, however, the SOC has no obvious influence on the density of carriers near the Fermi level. Thus, the critical value of T_K/Δ is shown close to a constant as usual [57].

IV. CONCLUSION

In this paper, we have studied the Kondo effect of a magnetic impurity doped in type-II Ising superconductors with multiple degenerate orbitals. The formation of a localized magnetic moment is shown anomalously extending to the doubly occupied region, and the phase boundary between magnetic and nonmagnetic states exhibits particle-hole asymmetry. We have demonstrated that the Ising-type SOC plays a role to suppress the Kondo effect, while the interorbital mixing effect in the bands enhances the Kondo screening. As a consequence, the QPT between magnetic doublet and KS ground states is significantly influenced by the band splitting near the Γ point. Accordingly, the Kondo screening of the magnetic moment can be tuned through the chemical potential. This motivates further experimental study using the magnetic impurity doped type-II Ising superconductors as a platform to explore the gate-tunable Kondo physics.

ACKNOWLEDGMENTS

This work was supported by the National Natural Science Foundation of China (Grants No. 11904234, No. 11874273, No. 12074108, No. 12147102, No. 11904245, No. 11834005 and No. 12047501), the Zhejiang Provincial Natural Science Foundation of China (Grant No. LY19A040003), the Postdoctoral Science Foundation of China (Grant No. 2021M690330), and the Natural Science Foundation of Chongqing (Grant No. CSTB2022NSCQ-MSX0568).

APPENDIX

In this Appendix, we present the main steps to obtain the impurity GF in the framework of HFA and Lacroix's treatment. The starting point is the equation of motion (EOM) of the retarded GF as follows [59]:

$$\omega\langle\langle A;B\rangle\rangle = \langle[A,B]_+\rangle + \langle\langle[A,H]_-;B\rangle\rangle, \tag{A1}$$

where the subscript $\pm$ stands for the anticommutation (commutation) relationship, and $\langle\langle A;B\rangle\rangle$ denotes the retarded GF composed by the operators A and B.

From the Hamiltonian Eq. (1) in main text, we obtain the EOM of the GFs composed of the creation (annihilation) operators of local and conduction electrons as

$$(\omega-\varepsilon_{d\sigma})\langle\langle d_\sigma;B\rangle\rangle = \langle[d_\sigma;B]_+\rangle + U\langle\langle d_\sigma n_{\bar\sigma};B\rangle\rangle + \sum_{km} V_0^*\langle\langle c_{km\sigma};B\rangle\rangle, \tag{A2}$$

$$(\omega-\varepsilon(k)-\sigma mM(k))\langle\langle c_{km\sigma};B\rangle\rangle = \sigma\Delta\langle\langle c^\dagger_{-k-m\bar\sigma};B\rangle\rangle + V_0\langle\langle d_\sigma;B\rangle\rangle, \tag{A3}$$

$$(\omega+\varepsilon(k)+\sigma mM(k))\langle\langle c^\dagger_{km\sigma};B\rangle\rangle = -\sigma\Delta\langle\langle c_{-k-m\bar\sigma};B\rangle\rangle - V_0^*\langle\langle d^\dagger_\sigma;B\rangle\rangle, \tag{A4}$$

and

$$(\omega+\varepsilon_{d\bar\sigma})\langle\langle d^\dagger_{\bar\sigma};B\rangle\rangle_\omega = \langle[d^\dagger_{\bar\sigma};B]_+\rangle - U\langle\langle d^\dagger_{\bar\sigma}n_\sigma;B\rangle\rangle - \sum_{km} V_0\langle\langle c^\dagger_{km\bar\sigma};B\rangle\rangle, \tag{A5}$$

where $\sigma(\bar\sigma)$ appearing in the coefficients is assumed to be ±1 for $\uparrow(\downarrow)$.

After some straightforward calculations and choosing the operator $B = d^\dagger_\sigma$ or $d_{\bar\sigma}$, we obtain the impurity GFs, which can be conveniently expressed in Nambu representation

$$\begin{pmatrix} \omega-\varepsilon_{d\sigma}-\hat\Sigma^0_{11\sigma}(\omega) & \hat\Sigma^0_{12\sigma}(\omega) \\ \hat\Sigma^0_{21\sigma}(\omega) & \omega+\varepsilon_{d\bar\sigma}-\hat\Sigma^0_{22\sigma}(\omega)\end{pmatrix}\begin{pmatrix}\langle\langle d_\sigma;d^\dagger_\sigma\rangle\rangle & \langle\langle d_\sigma;d_{\bar\sigma}\rangle\rangle \\ \langle\langle d^\dagger_{\bar\sigma};d^\dagger_\sigma\rangle\rangle & \langle\langle d^\dagger_{\bar\sigma};d_{\bar\sigma}\rangle\rangle\end{pmatrix} = \begin{pmatrix}1&0\\0&1\end{pmatrix} + U\begin{pmatrix}\langle\langle d_\sigma n_{\bar\sigma};d^\dagger_\sigma\rangle\rangle & \langle\langle d_\sigma n_{\bar\sigma};d_{\bar\sigma}\rangle\rangle \\ -\langle\langle d^\dagger_{\bar\sigma}n_\sigma;d^\dagger_\sigma\rangle\rangle & -\langle\langle d^\dagger_{\bar\sigma}n_\sigma;d_{\bar\sigma}\rangle\rangle\end{pmatrix}, \tag{A6}$$

where the noninteracting self-energy terms are given by

$$\hat\Sigma^0_{11\sigma}(\omega) = \frac{\Gamma_0}{\pi}\sum_{km}\frac{\omega+\varepsilon(k)+\sigma mM(k)}{\omega^2-[\varepsilon(k)+\sigma mM(k)]^2-\Delta^2}, \tag{A7}$$

$$\hat\Sigma^0_{22\sigma}(\omega) = \frac{\Gamma_0}{\pi}\sum_{km}\frac{\omega-\varepsilon(k)+\sigma mM(k)}{\omega^2-[\varepsilon(k)-\sigma mM(k)]^2-\Delta^2}, \tag{A8}$$

$$\hat{\Sigma}^0_{12\sigma}(\omega) = \frac{\Gamma_0}{\pi}\sum_{km}\frac{\Delta\sigma}{\omega^2-[\varepsilon(k)+\sigma mM(k)]^2-\Delta^2}, \quad \text{(A9)}$$

$$\hat{\Sigma}^0_{21\sigma}(\omega) = \frac{\Gamma_0}{\pi}\sum_{km}\frac{\sigma\Delta}{\omega^2-[\varepsilon(k)-\sigma mM(k)]^2-\Delta^2}, \quad \text{(A10)}$$

with the coupling strength $\Gamma_0(\omega)=\pi|V_0|^2$.

In Eq. (A6), the impurity GFs can be expressed by a concise form

$$\hat{G}_{d\sigma}(\omega) = \hat{G}^0_{d\sigma}(\omega) + U\hat{G}^0_{d\sigma}(\omega)\hat{F}_{d\sigma}(\omega), \quad \text{(A11)}$$

with

$$\left[\hat{G}^0_{d\sigma}(\omega)\right]^{-1} = \begin{pmatrix} \omega-\varepsilon_{d\sigma}-\hat{\Sigma}^0_{11\sigma}(\omega) & \hat{\Sigma}^0_{12\sigma}(\omega) \\ \hat{\Sigma}^0_{21\sigma}(\omega) & \omega+\varepsilon_{d\bar{\sigma}}-\hat{\Sigma}^0_{22\sigma}(\omega)\end{pmatrix}, \quad \text{(A12)}$$

and

$$\hat{F}_{d\sigma}(\omega) = \begin{pmatrix} \langle\langle d_\sigma n_{\bar{\sigma}}; d^\dagger_\sigma\rangle\rangle & \langle\langle d_\sigma n_{\bar{\sigma}}; d_{\bar{\sigma}}\rangle\rangle \\ -\langle\langle d^\dagger_{\bar{\sigma}} n_\sigma; d^\dagger_\sigma\rangle\rangle & -\langle\langle d^\dagger_{\bar{\sigma}} n_\sigma; d_{\bar{\sigma}}\rangle\rangle\end{pmatrix}. \quad \text{(A13)}$$

The notation $\hat{F}_{d\sigma}(\omega)$ includes some higher-order GFs. However, it is difficult to exactly calculate these GFs by the EOM approach, and one has to employ some approximation treatments. The HFA can be reached by taking the following approximations:

$$\langle\langle d_\sigma n_{\bar{\sigma}}; d^\dagger_\sigma\rangle\rangle \approx \langle n_{\bar{\sigma}}\rangle\langle\langle d_\sigma; d^\dagger_\sigma\rangle\rangle + \langle d_{\bar{\sigma}} d_\sigma\rangle\langle\langle d^\dagger_{\bar{\sigma}}; d^\dagger_\sigma\rangle\rangle, \quad \text{(A14)}$$

$$\langle\langle d_\sigma n_{\bar{\sigma}}; d_{\bar{\sigma}}\rangle\rangle \approx \langle n_{\bar{\sigma}}\rangle\langle\langle d_\sigma; d_{\bar{\sigma}}\rangle\rangle + \langle d_{\bar{\sigma}} d_\sigma\rangle\langle\langle d^\dagger_{\bar{\sigma}}; d_{\bar{\sigma}}\rangle\rangle, \quad \text{(A15)}$$

$$\langle\langle d^\dagger_{\bar{\sigma}} n_\sigma; d^\dagger_\sigma\rangle\rangle \approx \langle n_\sigma\rangle\langle\langle d^\dagger_{\bar{\sigma}}; d^\dagger_\sigma\rangle\rangle - \langle d^\dagger_\sigma d^\dagger_{\bar{\sigma}}\rangle\langle\langle d_\sigma; d^\dagger_\sigma\rangle\rangle, \quad \text{(A16)}$$

$$\langle\langle d^\dagger_{\bar{\sigma}} n_\sigma; d_{\bar{\sigma}}\rangle\rangle \approx \langle n_\sigma\rangle\langle\langle d^\dagger_{\bar{\sigma}}; d_{\bar{\sigma}}\rangle\rangle - \langle d^\dagger_\sigma d^\dagger_{\bar{\sigma}}\rangle\langle\langle d_\sigma; d_{\bar{\sigma}}\rangle\rangle. \quad \text{(A17)}$$

Then, we obtain

$$\hat{F}_{d\sigma}(\omega) = \begin{pmatrix} \langle n_{\bar{\sigma}}\rangle & \langle d_{\bar{\sigma}} d_\sigma\rangle \\ \langle d^\dagger_\sigma d^\dagger_{\bar{\sigma}}\rangle & -\langle n_\sigma\rangle\end{pmatrix}\begin{pmatrix} \langle\langle d_\sigma; d^\dagger_\sigma\rangle\rangle & \langle\langle d_\sigma; d_{\bar{\sigma}}\rangle\rangle \\ \langle\langle d^\dagger_{\bar{\sigma}}; d^\dagger_\sigma\rangle\rangle & \langle\langle d^\dagger_{\bar{\sigma}}; d_{\bar{\sigma}}\rangle\rangle\end{pmatrix}, \quad \text{(A18)}$$

and the impurity GFs can be read,

$$\hat{G}_{d\sigma}(\omega) = \hat{G}^0_{d\sigma}(\omega) + \hat{G}^0_{d\sigma}(\omega)\hat{\Sigma}^{\rm HF}_\sigma(\omega)\hat{G}_{d\sigma}(\omega), \quad \text{(A19)}$$

with the interacting self-energy

$$\hat{\Sigma}^{\rm HF}_\sigma(\omega) = U\begin{pmatrix} \langle n_{\bar{\sigma}}\rangle & \langle d_{\bar{\sigma}} d_\sigma\rangle \\ \langle d^\dagger_\sigma d^\dagger_{\bar{\sigma}}\rangle & -\langle n_\sigma\rangle\end{pmatrix}, \quad \text{(A20)}$$

where the occupation of impurity level is given by $\langle n_{\bar{\sigma}}\rangle = -\frac{1}{\pi}\int f(\omega){\rm Im}[\hat{G}_{d\bar{\sigma}}(\omega)]_{11}d\omega$, $f(\omega)$ is the Fermi distribution function, and $\langle d^\dagger_\sigma d^\dagger_{\bar{\sigma}}\rangle = -\frac{1}{\pi}\int f(\omega){\rm Im}[\hat{G}_{d\sigma}(\omega)]_{21}d\omega$ is the pairing correlation function. Then, the diagonal part of the GF can be explicitly written as

$$[\hat{G}_{d\sigma}(\omega)]_{11} = \frac{1}{\omega-\varepsilon_{d\sigma}-\hat{\Sigma}^0_{11\sigma}(\omega)-U\langle n_{\bar{\sigma}}\rangle+\hat{\Sigma}^0_{12\sigma}(\omega)\Theta_\sigma(\omega)}, \quad \text{(A21)}$$

and the anomalous part reads

$$[\hat{G}_{d\sigma}(\omega)]_{21} = \Theta_\sigma(\omega)[\hat{G}_{d\sigma}(\omega)]_{11}, \quad \text{(A22)}$$

where the notation

$$\Theta_\sigma(\omega) = \frac{U\langle d^\dagger_\sigma d^\dagger_{\bar{\sigma}}\rangle - \hat{\Sigma}^0_{21\sigma}(\omega)}{\omega+\varepsilon_{d\bar{\sigma}}+U\langle n_\sigma\rangle-\hat{\Sigma}^0_{22\sigma}(\omega)}. \quad \text{(A23)}$$

With the above formulas, one can discuss the QPT between the BCS-singlet and the magnetic doublet ground states in the frame of HFA [39–42].

To capture the Kondo physics, we must treat the high-order GF $\langle\langle d_\sigma n_{\bar{\sigma}}; d^\dagger_\sigma\rangle\rangle$ by using the EOM method as follows:

$$(\omega-\varepsilon_{d\sigma}-U)\langle\langle d_\sigma n_{\bar{\sigma}}; d^\dagger_\sigma\rangle\rangle = \langle n_{\bar{\sigma}}\rangle + \sum_{km}V_0(\langle\langle c_{km\sigma}n_{\bar{\sigma}}; d^\dagger_\sigma\rangle\rangle - \langle\langle c^\dagger_{km\bar{\sigma}}d_{\bar{\sigma}}d_\sigma; d^\dagger_\sigma\rangle\rangle) + \sum_{km}V^*_0\langle\langle d^\dagger_{\bar{\sigma}}c_{km\bar{\sigma}}d_\sigma; d^\dagger_\sigma\rangle\rangle. \quad \text{(A24)}$$

The EOMs of the higher-order GFs produced in Eq. (A24) are given by

$$\begin{aligned}(\omega-\varepsilon_{1m\sigma k})\langle\langle c_{km\sigma}n_{\bar{\sigma}}; d^\dagger_\sigma\rangle\rangle &= \sum_{k'm'}(V^*_0\langle\langle d^\dagger_{\bar{\sigma}}c_{k'm'\bar{\sigma}}c_{km\sigma}; d^\dagger_\sigma\rangle\rangle - V_0\langle\langle c^\dagger_{k'm'\bar{\sigma}}d_{\bar{\sigma}}c_{km\sigma}; d^\dagger_\sigma\rangle\rangle) \\ &\quad + V_0\langle\langle d_\sigma n_{\bar{\sigma}}; d^\dagger_\sigma\rangle\rangle + \sigma\Delta\langle\langle c^\dagger_{-k-m\bar{\sigma}}n_{\bar{\sigma}}; d^\dagger_\sigma\rangle\rangle, \quad \text{(A25)}\end{aligned}$$

$$\begin{aligned}(\omega-\varepsilon_{2m\sigma k})\langle\langle d^\dagger_{\bar{\sigma}}c_{km\bar{\sigma}}d_\sigma; d^\dagger_\sigma\rangle\rangle &= \sum_{k'm'}(V^*_0\langle\langle d^\dagger_{\bar{\sigma}}c_{km\bar{\sigma}}c_{k'm'\sigma}; d^\dagger_\sigma\rangle\rangle - V_0\langle\langle c^\dagger_{k'm'\bar{\sigma}}c_{km\bar{\sigma}}d_\sigma; d^\dagger_\sigma\rangle\rangle) + V_0\langle\langle d_\sigma n_{\bar{\sigma}}; d^\dagger_\sigma\rangle\rangle \\ &\quad + \langle d^\dagger_{\bar{\sigma}}c_{km\bar{\sigma}}\rangle - \sigma\Delta\langle\langle d^\dagger_{\bar{\sigma}}c^\dagger_{-k-m\sigma}d_\sigma; d^\dagger_\sigma\rangle\rangle, \quad \text{(A26)}\end{aligned}$$

and

$$\begin{aligned}(\omega-\varepsilon_{3m\sigma k})\langle\langle c^\dagger_{km\bar{\sigma}}d_{\bar{\sigma}}d_\sigma; d^\dagger_\sigma\rangle\rangle &= \sum_{k'm'}V^*_0(\langle\langle c^\dagger_{km\bar{\sigma}}d_{\bar{\sigma}}c_{k'm'\sigma}; d^\dagger_\sigma\rangle\rangle + \langle\langle c^\dagger_{km\bar{\sigma}}c_{k'm'\bar{\sigma}}d_\sigma; d^\dagger_\sigma\rangle\rangle) - V^*_0\langle\langle d_\sigma n_{\bar{\sigma}}; d^\dagger_\sigma\rangle\rangle \\ &\quad + \langle c^\dagger_{km\bar{\sigma}}d_{\bar{\sigma}}\rangle + \sigma\Delta\langle\langle c_{-k-m\sigma}d_{\bar{\sigma}}d_\sigma; d^\dagger_\sigma\rangle\rangle, \quad \text{(A27)}\end{aligned}$$

with $\varepsilon_{1m\sigma k} = \varepsilon(k) - m\sigma M(k)$, $\varepsilon_{2m\sigma k} = \varepsilon(k) - m\sigma M(k) + \varepsilon_{d\sigma} - \varepsilon_{d\bar{\sigma}}$, and $\varepsilon_{3m\sigma k} = -\varepsilon(k) + m\sigma M(k) + \varepsilon_{d\sigma} + \varepsilon_{d\bar{\sigma}} + U$.

In the above equations, the impurity-superconducting correlation terms, such as $\Delta\langle\langle c^\dagger_{-k\bar{\sigma}}n_{\bar{\sigma}}; d^\dagger_\sigma\rangle\rangle$, $\Delta\langle\langle c^\dagger_{-k\sigma}d_\sigma d^\dagger_{\bar{\sigma}}; d^\dagger_\sigma\rangle\rangle$, and

$\Delta\langle\langle c_{-k\sigma}d_{\bar{\sigma}}d_{\sigma};d_{\sigma}^{\dagger}\rangle\rangle$ are believed to be much weaker than other terms. Thus, we can safely neglect these terms in the above equations.

To capture the Kondo physics, we take the Lacroix's approximation to treat the higher-order GFs in Eqs. (A25)–(A27). The Lacroix's scheme can be reached by taking the decoupling procedures:

$$\langle\langle d_{\bar{\sigma}}^{\dagger}c_{k'm'\bar{\sigma}}c_{km\sigma};d_{\sigma}^{\dagger}\rangle\rangle \approx \langle d_{\bar{\sigma}}^{\dagger}c_{k'm'\bar{\sigma}}\rangle\langle\langle c_{km\sigma};d_{\sigma}^{\dagger}\rangle\rangle, \quad \text{(A28)}$$

$$\langle\langle c_{k'm'\bar{\sigma}}^{\dagger}d_{\bar{\sigma}}c_{km\sigma};d_{\sigma}^{\dagger}\rangle\rangle \approx \langle c_{k'm'\bar{\sigma}}^{\dagger}d_{\bar{\sigma}}\rangle\langle\langle c_{km\sigma};d_{\sigma}^{\dagger}\rangle\rangle, \quad \text{(A29)}$$

$$\langle\langle d_{\bar{\sigma}}^{\dagger}c_{km\bar{\sigma}}c_{k'm'\sigma};d_{\sigma}^{\dagger}\rangle\rangle \approx \langle d_{\bar{\sigma}}^{\dagger}c_{km\bar{\sigma}}\rangle\langle\langle c_{k'm'\sigma};d_{\sigma}^{\dagger}\rangle\rangle, \quad \text{(A30)}$$

$$\langle\langle c_{k'm'\bar{\sigma}}^{\dagger}c_{km\bar{\sigma}}d_{\sigma};d_{\sigma}^{\dagger}\rangle\rangle \approx \langle c_{k'm'\bar{\sigma}}^{\dagger}c_{km\bar{\sigma}}\rangle\langle\langle d_{\sigma};d_{\sigma}^{\dagger}\rangle\rangle, \quad \text{(A31)}$$

$$\langle\langle c_{km\bar{\sigma}}^{\dagger}d_{\bar{\sigma}}c_{k'm'\sigma};d_{\sigma}^{\dagger}\rangle\rangle \approx \langle c_{km\bar{\sigma}}^{\dagger}d_{\bar{\sigma}}\rangle\langle\langle c_{k'm'\sigma};d_{\sigma}^{\dagger}\rangle\rangle, \quad \text{(A32)}$$

$$\langle\langle c_{km\bar{\sigma}}^{\dagger}c_{k'm'\bar{\sigma}}d_{\sigma};d_{\sigma}^{\dagger}\rangle\rangle \approx \langle c_{km\bar{\sigma}}^{\dagger}c_{k'm'\bar{\sigma}}\rangle\langle\langle d_{\sigma};d_{\sigma}^{\dagger}\rangle\rangle. \quad \text{(A33)}$$

Then, we obtain

$$\begin{aligned}&(\omega-\varepsilon_{1m\sigma k})\langle\langle c_{km\sigma}n_{\bar{\sigma}};d_{\sigma}^{\dagger}\rangle\rangle\\&=\sum_{k'm'}(V_0^{*}\langle d_{\bar{\sigma}}^{\dagger}c_{k'm'\bar{\sigma}}\rangle-V_0\langle c_{k'm'\bar{\sigma}}^{\dagger}d_{\bar{\sigma}}\rangle)\langle\langle c_{km\sigma};d_{\sigma}^{\dagger}\rangle\rangle\\&\quad+\sigma\Delta\langle\langle c_{-k-m\bar{\sigma}}^{\dagger}n_{\bar{\sigma}};d_{\sigma}^{\dagger}\rangle\rangle_{\omega}+V_0\langle\langle d_{\sigma}n_{\bar{\sigma}};d_{\sigma}^{\dagger}\rangle\rangle, \quad \text{(A34)}\end{aligned}$$

$$\begin{aligned}&(\omega-\varepsilon_{2m\sigma k})\langle\langle d_{\bar{\sigma}}^{\dagger}c_{km\bar{\sigma}}d_{\sigma};d_{\sigma}^{\dagger}\rangle\rangle\\&=\sum_{k'm'}[V_0^{*}\langle d_{\bar{\sigma}}^{\dagger}c_{km\bar{\sigma}}\rangle\langle\langle c_{k'm'\sigma};d_{\sigma}^{\dagger}\rangle\rangle-V_0\langle c_{k'm'\bar{\sigma}}^{\dagger}c_{km\bar{\sigma}}\rangle\langle\langle d_{\sigma};d_{\sigma}^{\dagger}\rangle\rangle]\\&\quad+\langle d_{\bar{\sigma}}^{\dagger}c_{km\bar{\sigma}}\rangle+V_0\langle\langle n_{\bar{\sigma}}d_{\sigma};d_{\sigma}^{\dagger}\rangle\rangle-\sigma\Delta\langle\langle d_{\bar{\sigma}}^{\dagger}c_{-k-m\sigma}^{\dagger}d_{\sigma};d_{\sigma}^{\dagger}\rangle\rangle, \quad \text{(A35)}\end{aligned}$$

and

$$\begin{aligned}&(\omega-\varepsilon_{3m\sigma k})\langle\langle c_{km\bar{\sigma}}^{\dagger}d_{\bar{\sigma}}d_{\sigma};d_{\sigma}^{\dagger}\rangle\rangle\\&=\sum_{k'm'}V_0^{*}(\langle c_{km\bar{\sigma}}^{\dagger}d_{\bar{\sigma}}\rangle\langle\langle c_{k'm'\sigma};d_{\sigma}^{\dagger}\rangle\rangle+\langle c_{km\bar{\sigma}}^{\dagger}c_{k'm'\bar{\sigma}}\rangle\langle\langle d_{\sigma};d_{\sigma}^{\dagger}\rangle\rangle)\\&+\langle c_{km\bar{\sigma}}^{\dagger}d_{\bar{\sigma}}\rangle-V_0^{*}\langle\langle d_{\sigma}n_{\bar{\sigma}};d_{\sigma}^{\dagger}\rangle\rangle_{\omega}+\sigma\Delta\langle\langle c_{-k-m\sigma}d_{\bar{\sigma}}d_{\sigma};d_{\sigma}^{\dagger}\rangle\rangle. \quad \text{(A36)}\end{aligned}$$

By taking some straightforward calculations, we obtain

$$\langle\langle d_{\sigma}n_{\bar{\sigma}};d_{\sigma}^{\dagger}\rangle\rangle_{\omega}=\Lambda_{\sigma}(\omega)+\Phi_{\sigma}(\omega)\langle\langle d_{\sigma};d_{\sigma}^{\dagger}\rangle\rangle_{\omega}, \quad \text{(A37)}$$

with

$$\Lambda_{\sigma}(\omega)=\frac{\langle n_{\bar{\sigma}}\rangle+[\Pi_{2\sigma}(\omega)-\Pi_{3\sigma}(\omega)]}{\omega-\varepsilon_{d\sigma}-U-\Xi_{1\sigma}(\omega)-\Xi_{2\sigma}(\omega)-\Xi_{3\sigma}(\omega)} \quad \text{(A38)}$$

and

$$\Phi_{\sigma}(\omega)=\frac{[\Pi_{2\sigma}(\omega)-\Pi_{3\sigma}(\omega)]\hat{\Sigma}_{11\sigma}^{0}(\omega)-[\Omega_{2\sigma}(\omega)+\Omega_{3\sigma}(\omega)]}{\omega-\varepsilon_{d\sigma}-U-\Xi_{1\sigma}(\omega)-\Xi_{2\sigma}(\omega)-\Xi_{3\sigma}(\omega)}. \quad \text{(A39)}$$

Finally, we gain the diagonal part of the impurity GF written as

$$[\hat{G}_{d\sigma}(\omega)]_{11}=\frac{1+U\Lambda_{\sigma}(\omega)}{\omega-\varepsilon_{d\sigma}-\hat{\Sigma}_{11\sigma}^{0}(\omega)-U\Phi_{\sigma}(\omega)+\Theta_{\sigma}(\omega)}. \quad \text{(A40)}$$

The notations involved in Eqs. (A38) and (A39) are given by $\Xi_{i\sigma}(\omega)=\frac{\Gamma_0}{\pi}\sum_{km}\frac{1}{\omega-\varepsilon_{im\sigma k}}$, $\Pi_{i\sigma}(\omega)=\sum_{km}\frac{V_0\langle d_{\bar{\sigma}}^{\dagger}c_{km\bar{\sigma}}\rangle}{\omega-\varepsilon_{im\sigma k}}$, and $\Omega_{i\sigma}(\omega)=\sum_{km}\sum_{k'm'}\frac{|V_0|^2\langle c_{km\bar{\sigma}}^{\dagger}c_{k'm'\bar{\sigma}}\rangle}{\omega-\varepsilon_{im\sigma k}}$. The value of $\langle d_{\bar{\sigma}}^{\dagger}c_{km\bar{\sigma}}\rangle$ and $\langle c_{km\bar{\sigma}}^{\dagger}c_{k'm'\bar{\sigma}}\rangle$ can be obtained by the spectral theorem

$$\langle d_{\bar{\sigma}}^{\dagger}c_{km\bar{\sigma}}\rangle=-\frac{1}{\pi}\int f(\omega)\mathrm{Im}\langle\langle c_{km\bar{\sigma}};d_{\bar{\sigma}}^{\dagger}\rangle\rangle d\varepsilon \quad \text{(A41)}$$

and

$$\langle c_{km\bar{\sigma}}^{\dagger}c_{k'm'\bar{\sigma}}\rangle=-\frac{1}{\pi}\int f(\omega)\mathrm{Im}\langle\langle c_{k'm'\bar{\sigma}};c_{km\bar{\sigma}}^{\dagger}\rangle\rangle d\varepsilon. \quad \text{(A42)}$$

The GFs $\langle\langle c_{km\bar{\sigma}};d_{\bar{\sigma}}^{\dagger}\rangle\rangle$ and $\langle\langle c_{k'm'\bar{\sigma}};c_{km\bar{\sigma}}^{\dagger}\rangle\rangle$ can be calculated by using Eqs. (A2)–(A5), then we obtain

$$\Pi_{i\sigma}(\omega)=\frac{\Gamma_0}{\pi}\sum_{km}\frac{\phi_{m\sigma}(k)}{\omega-\varepsilon_{im\sigma k}} \quad \text{(A43)}$$

and

$$\Omega_{i\sigma}(\omega)=\frac{\Gamma_0}{\pi}\sum_{km}\frac{\varphi_{m\sigma}(k)}{\omega-\varepsilon_{im\sigma k}}, \quad \text{(A44)}$$

with

$$\phi_{m\sigma}(k)=\frac{-1}{\pi}\int d\omega f(\omega)\mathrm{Im}\frac{[\omega+\varepsilon(k)-\sigma mM(k)][\hat{G}_{d\bar{\sigma}}(\omega)]_{11}}{\omega^2-[\varepsilon(k)-\sigma mM(k)]^2-\Delta^2} \quad \text{(A45)}$$

and

$$\varphi_{m\sigma}(k)=\frac{-1}{\pi}\int d\omega f(\omega)\mathrm{Im}\frac{\omega+\varepsilon(k)-m\sigma M(k)}{\omega^2-[\varepsilon(k)-\sigma mM(k)]^2-\Delta^2}. \quad \text{(A46)}$$

[1] Q. Y. Wang, Z. Li, W. H. Zhang, Z. C. Zhang, J. S. Zhang, W. Li, H. Ding, Y. B. Ou, P. Deng, K. Chang, J. Wen, C. L. Song, K. He, J. F. Jia, S. H. Ji, Y. Y. Wang, L. L. Wang, X. Chen, X. C. Ma, and Q. K. Xue, Chin. Phys. Lett. **29**, 037402 (2012).

[2] J. M. Lu, O. Zeliuk, I. Leemakers, Naoh F. Q. Yuan, U. Zeitler, K. T. Law, and J. T. Ye, Science **350**, 1353 (2015).

[3] X. Xi, Z. Wang, W. Zhao, J. H. Park, K. T. Low, H. Berger, L. Folló, J. Shan, and K. F. Mak, Nat. Phys. **12**, 139 (2016).

[4] Y. Saito, Y. Nakamura, M. S. Bahramy, Y. Kohama, J. T. Ye, Y. Kasahara, Y. Nakagawa, M. Onga, M. Tokunaga, T. Nojima, Y. Yanase, and Y. Iwasa, Nat. Phys. **12**, 144 (2016).

[5] P. Zhang, K. Yaji, T. Hashinoto, Y. Ota, T. Kondo, K. Okazaki, Z. J. Wang, J. S. Wen, G. D. Gu, H. Ding, and S. Shin, Science **360**, 182 (2018).

[6] Z. Chen, Y. Liu, H. Zhang, Z. R. Liu, H. Tian, Y. Q. Sun, M. Zhang, Y. Zhou, J. R. Sun, and Y. W. Xie, Science **372**, 721 (2021).

[7] M. Sadovskii, Phys. Rep. **282**, 225 (1997).
[8] B. G. Orr, H. M. Jaeger, and A. M. Goldman, Phys. Rev. Lett. **53**, 2046 (1984).
[9] J. M. Blatt and C. J. Thompson, Phys. Rev. Lett. **10**, 332 (1963).
[10] V. L. Berezinskii, Zh. Eksp. Teor. Fiz. **61**, 1144 (1972) [Sov. Phys. JETP **34**, 610 (1972)].
[11] J. M. Kosterlitz and D. J. Thouless, J. Phys. C **6**, 1181 (1973).
[12] Y. Xing, K. Zhao, P. Shan, F. Zheng, Y. Zhang, H. Fu, Y. Liu, M. Tian, C. Xi, H. Liu, J. Feng, X. Lin, S. Ji, X. Chen, Q.-K. Xue, and J. Wang, Nano Lett. **17**, 6802 (2017).
[13] J. M. Lu, O. Zheliuk, Q. H. Chen, I. Leermakers, N. E. Hussey, U. Zeitler, and J. T. Ye, PNAS **115**, 3551 (2018).
[14] C. Wang, B. Lian, X. M. Guo, J. H. Mao, Z. T. Zhang, D. Zhang, B. L. Gu, Y. Xu, and W. H. Duan, Phys. Rev. Lett. **123**, 126402 (2019).
[15] J. Falson, Y. Xu, M. H. Liao, Y. Y. Zang, K. J. Zhu, C. Wang, Z. T. Zhang, H. C. Liu, W. H. Duan, K. He, H. W. Liu, J. H. Smet, D. Zhang, and Q. K. Xue, Science **367**, 1454 (2020).
[16] Y. Liu, Y. Xu, J. Sun, C. Liu, Y. Z. Liu, C. Wang, Z. T. Zhang, K. Y. Gu, Y. Tang, C. Ding, H. W. Liu, H. Yao, X. Lin, L. L. Wang, Q. K. Xue, and J. Wang, Nano Lett. **20**, 5728 (2020).
[17] M. E. Flatté and J. M. Byers, Phys. Rev. Lett. **78**, 3761 (1997).
[18] A. Yazdani, B. A. Jones, C. P. Lutz, M. F. Crommie, and D. M. Eigler, Science **275**, 1767 (1997).
[19] A. V. Balatsky, I. Vekhter, and J. X. Zhu, Rev. Mod. Phys. **78**, 373 (2006).
[20] K. J. Franke, G. Schulze, and J. I. Pascual, Science **332**, 940 (2011).
[21] Y. Luh, Acta Phys. Sin. **21**, 75 (1965).
[22] H. Shiba, Prog. Theor. Phys. **40**, 435 (1968).
[23] A. I. Rusinov, Zh. Eksp. Teor. Fiz. **56**, 2047 (1969) [Sov. Phys. JETP **29**, 1101 (1969)].
[24] A. A. Clerk and V. Ambegaokar, Phys. Rev. B **61**, 9109 (2000).
[25] G. Sellier, T. Kopp, J. Kroha, and Y. S. Barash, Phys. Rev. B **72**, 174502 (2005).
[26] C. Buizert, A. Oiwa, K. Shibata, K. Hirakawa, and S. Tarucha, Phys. Rev. Lett. **99**, 136806 (2007).
[27] E. J. H. Lee, X. Jiang, R. Aguado, G. Katsaros, C. M. Lieber, and S. De Franceschi, Phys. Rev. Lett. **109**, 186802 (2012).
[28] W. Chang, V. E. Manucharyan, T. S. Jespersen, J. Nygard, and C. M. Marcus, Phys. Rev. Lett. **110**, 217005 (2013).
[29] B. K. Kim, Y. H. Ahn, J. J. Kim, M. S. Choi, M. H. Bae, K. Kang, J. S. Lim, R. López, and N. Kim, Phys. Rev. Lett. **110**, 076803 (2013).
[30] J. O. Island, R. Gaudenzi, J. de Bruijckere, E. Burzuri, C. Franco, M. Mas-Torrent, C. Rovira, J. Veciana, T. M. Klapwijk, R. Aguado, and H. S. J. van der Zant, Phys. Rev. Lett. **118**, 117001 (2017).
[31] A. C. Hewson, *The Kondo Problem to Heavy Fermions* (Cambridge University Press, Cambridge, UK, 1993).
[32] L. Li, B. B. Zheng, W. Q. Chen, H. Chen, H. G. Luo, and F. C. Zhang, Phys. Rev. B **89**, 245135 (2014).
[33] M. Phillips and V. Aji, Phys. Rev. B **95**, 075103 (2017).
[34] G. Sharma and S. Tewari, Phys. Rev. B **94**, 094515 (2016).
[35] Y. Zhang, L. Li, J. H. Sun, D. H. Xu, R. Lu, and H. G. Luo, and W. Q. Chen, Phys. Rev. B **101**, 035124 (2020).
[36] J. Zhang and V. Aji, Phys. Rev. B **94**, 060501(R) (2016).
[37] P. W. Anderson, Phys. Rev. **124**, 41 (1961).
[38] B. Uchoa, V. N. Kotov, N. M. R. Peres, and A. H. Castro Neto, Phys. Rev. Lett. **101**, 026805 (2008); **101**, 039903(E) (2008).
[39] E. J. H. Lee, X. C. Jia, M. Houzet, R. Aguado, C. M. Lieber, and S. D. Franceschi, Nat. Nanotechnol. **9**, 79 (2014).
[40] E. Vecino, A. Martín-Rodero, and A. Levy Yeyati, Phys. Rev. B **68**, 035105 (2003).
[41] J. C. Cuevas, A. Levy Yeyati, and A. Martin-Rodero, Phys. Rev. B **63**, 094515 (2001).
[42] C. Benjamin, T. Jonckheere, A. Zazunov, and T. Martin, Eur. Phys. J. B **57**, 279 (2007).
[43] C. Lacroix, J. Phys. F **11**, 2389 (1981).
[44] H.-G. Luo, Z.-J. Ying, and S.-J. Wang, Phys. Rev. B **59**, 9710 (1999).
[45] M. Krawiec and K. I. Wysokiński, Supercond. Sci. Technol. **17**, 103 (2004).
[46] S.-Y. Shiau, S. Chutia, and R. Joynt, Phys. Rev. B **75**, 195345 (2007).
[47] T. Domański, A. Donabidowicz, and K. I. Wysokiński, Phys. Rev. B **78**, 144515 (2008).
[48] Y. Qi, J.-X. Zhu, S. Zhang, and C. S. Ting, Phys. Rev. B **78**, 045305 (2008).
[49] Q. Feng, Y.-Z. Zhang, and H. O. Jeschke, Phys. Rev. B **79**, 235112 (2009).
[50] T.-F. Fang, W. Zuo, and H.-G. Luo, Phys. Rev. Lett. **101**, 246805 (2008); **104**, 169902(E) (2010).
[51] J. Barański and T. Domański, Phys. Rev. B **84**, 195424 (2011).
[52] D. Krychowski, J. Kaczkowski, and S. Lipinski, Phys. Rev. B **89**, 035424 (2014).
[53] L. Li, Z. Cao, T. F. Fang, H. G. Luo, and W. Q. Chen, Phys. Rev. B **94**, 165144 (2016).
[54] L. Li, M. X. Gao, Z. H. Wang, H. G. Luo, and W. Q. Chen, Phys. Rev. B **97**, 064519 (2018).
[55] T. Meng, S. Florens, and P. Simon, Phys. Rev. B **79**, 224521 (2009).
[56] L. Li, J. H. Sun, Z. H. Wang, D. H. Xu, H. G. Luo, and W. Q. Chen, Phys. Rev. B **98**, 075110 (2018).
[57] F. Siano and R. Egger, Phys. Rev. Lett. **93**, 047002 (2004); **94**, 039902(E) (2005).
[58] F. D. M. Haldane, Phys. Rev. Lett. **40**, 416 (1978).
[59] D. N. Zubarev, Usp. Fiz. Nauk **71**, 71 (1960) [Sov. Phys. Usp. **3**, 320 (1960)].